

Regular Article

Developing Uplink Power Optimization and ARS Selection Algorithm for Multi-ARS Small Cell Communication System

Be Thi Bich Hoai, Bui Anh Duc, Pham Thanh Hiep, Nguyen Thu Phuong

Faculty of Radio Electronics Engineering, Le Quy Don Technical University, Ha Noi, Viet Nam

Correspondence: Nguyen Thu Phuong, phuong.nt@mta.edu.vn

Communication: received 13 November 2023, revised 24 December 2023, accepted 31 December 2023

Online publication: 02 January 2024, Digital Object Identifier: 10.21553/rev-jec.342

The associate editor coordinating the review of this article and recommending it for publication was Prof. Hoang Van Phuc.

Abstract– A well-prepared abstract enables the reader to Small Cell (SC) models and unmanned aerial vehicles (UAVs) acting as aerial relay stations (ARSs) are both promising advancements in the development of upcoming wireless networks that contribute significantly to improving the overall service quality. In this work, we rely on the Multi-ARS Cell-Free (CF) model, where a large number of ARS coordinated by the ground base station (GBS) and cooperate to serve a large number of users within the same frequency and time resources, to develop the uplink of a multi-ARS SC system, in which each user is served by only one ARS. The time division duplex (TDD) mechanism is used for the communication protocol, and the Minimum Mean Square Error (MMSE) method is implemented to estimate the uplink channel. We derive a closed-form expression for uplink user throughput. In addition, we introduce the ARS selection method based on channel conditions and propose the Bisection algorithm to optimize uplink power. The system performance is evaluated by the cumulative distribution function (CDF) of user throughput according to different parameters, such as the number of ARS, the number of users, the number of antennas, and the length of pilot sequences with/without power optimization. The results reveal that the ARS selection method is effectively resolved to reduce complexity and improve the practicality of the proposed system, and the power optimization problem brings better throughput than non-optimization.

Keywords– Small cell, multi-ARS, power optimization, ARS selection.

1 INTRODUCTION

Wireless technology has undergone a significant evolution since inception. The future of wireless technology is promising with the development of 5G networks, the Internet of Things (IoT), and artificial intelligence (AI). Advanced communication systems make a manifold increase in the number of interconnected devices, offer high-speed data transmission capabilities, near real-time responsiveness [1]. The rapid development and widespread adoption of 5G technology have promoted the design of wireless systems beyond 5G (B5G), which requires a higher network density and mobile data usage than previously seen. To meet the requirements of advanced communication systems, Small Cell (SC) geometry is being considered to improve coverage and capacity in dense urban [2].

The SC models consist of low-power cellular access nodes which play a vital role in the architecture of 5G wireless networks. These nodes are designed to enhance network coverage and capacity in areas with high network traffic or limited coverage. As compared to traditional cellular towers, SC is more cost-effective, requires less space and consumes less power [3]. Effective SC deployment scenarios were examined in terms of signal-to-interference-plus-noise ratio (SINR) performance by Pak et al. [4]. The complexity of the deployment problem is increased by cross-cell interference (between the macrocells and small cells) and inter-cell interference (between small cells), which remains a sig-

nificant obstacle for the SC deployment. Moreover, the implementation of the SC model suffers from a major handover problem between cells [5]. 5G mobility management in ultra-dense small cells (UDSC) networks using reinforcement learning techniques especially handover (HO) management in UDSC scenario has been studied and addressed the problem concisely [6].

With the ability to operate at high altitudes and adapt to changing environmental conditions, ARSs systems offer a unique platform for enhancing the performance of wireless networks and providing users with a seamless, high-quality experience [7]. The utilization of ARSs allows the greater spatial and time diversity of the wireless signals. The integration of ARSs communication and the SC models is a promising solution for enhancing the coverage and quality of service in high mobility environments and presents an innovative opportunity for the communications technology industry.

The base stations of current cellular networks are lack of flexibility and maneuverability. To address the limitations, various technologies have been proposed in the literature, and the use of ARSs communication has emerged as a promising solution. Using ARSs offers several benefits for terrestrial networks, such as cost-effectiveness, efficient coverage of a large area, reliable coordination with ground communication devices, a robust backup network [8]. ARSs are proving to be more effective than terrestrial relay stations in various scenarios [9]. This is possible because ARSs are mobile, flexible, and can access unreachable locations, increas-

ing the Line-of-Sight (LoS) probability [10]. The practical matters such as analyzing the deployment, performance, resource management, trajectory optimization, channel modeling, and realizing aerial base stations have been carefully examined [11]. A framework utilizing stochastic geometry was presented to analyze downlink coverage and ergodic capacity in an ARS-assisted millimeter-wave cellular network [12].

In this paper, we present a novel SC model that eliminates the "cell" concept and its negative impacts by relying on the CF model. Simultaneously, ARSs are utilized in our model to achieve better channel conditions and enhance the system's flexibility.

1.1 Motivation

From surveying the status of research that has been carried out in the field of the SC and ARSs, we see that combining the SC and ARSs is a new research direction with great practical potential for the following reasons:

Firstly, although the conventional SC model brings great efficiency in improving system quality, the model faces to the problem of cell-to-cell handover and high interference among cells when the number of separate small cells grows too large. To address the issues, there is a need for a new approach to advance the conventional SC model. One possible solution is to move away from the concept of "cells" and adopt a more flexible approach to network design.

Secondly, the integration of the ARSs and the SC model is a relatively new research area that has not been extensively explored, especially, a completely new SC model, which is developed taking into account the absence of "cells" concept as CF models. Combining ARS and the SC technology can create a new model that offers several advantages over traditional wireless communication systems including a high probability of LoS communication, adaptable deployment, and efficient signal processing.

Finally, one of the most particularly important problems is power optimization, especially with the advent of the ARS communication. The primary goals of power optimization are to minimize interference between different network components and extend the lifespan of wireless networks.

1.2 Contribution

Summary of the principal contributions of this paper follows as:

- We develop the uplink SC model based on the CF system [13], in which each user is served by a single ARS. ARSs select users based on optimal channel conditions for effective communication.
- We design the channel model according to the standard for Enhanced LTE Support for Aerial Vehicles provided by International Telecommunication Union (ITU) and Generation Partnership Project (3GPP) [14]. The TDD protocol is applied, and the MMSE method is used for the uplink channel estimation.

- We determine the closed-form expression for the system in terms of the uplink throughput and present a strategy for optimizing the power coefficient of the uplink.
- We evaluate system performance by comparing the throughput achieved per user with and without optimization. This evaluation is performed by examining the impact of system parameters, including the number of ARS, the number of antennas per ARS, the number of users, and the length of the pilot sequences.

The rest of paper is organized as follows. In Section 2, we describe the SC multi-ARS system model. The uplink data transmission and ARS selection problems will be solved in Section 3. Section 4 presents uplink power the optimization problem. Section 5 brings the numerical results and accompanying remarks, while the conclusion is presented in Section 6. For ease of reference, Table I has been organized to display the mathematical symbols's notations.

Table I
MATHEMATICAL SYMBOLS IN THIS PAPER

Notation	Description
$(\cdot)^*$	Conjugate
$(\cdot)^H$	Conjugate-Transpose
$\mathbb{E}\{\cdot\}$	Expectation operator
$\ \cdot\ $	The Euclidean norm
\mathbf{I}_N	The $N \times N$ identity matrix
$\mathbf{C}^{m \times n}$	A vector or matrix with size of $m \times n$
η_k^u	Uplink data power control coefficient
η_k	Pilot power control coefficient
K	Number of Users
M	Number of antennas at ARS
A	Number of ARSs

2 SYSTEM MODEL

We first deploy the Multi-ARS CF system with A ARSs and K terrestrial users ($K < A$) [13], as displayed in Figure 1. All ARSs are equipped with M antenna while all users are equipped with a single antenna. They are randomly located in a large area ($S \text{ km}^2$). Moreover, ARSs are connected to the ground base station (GBS) through an ideal backhaul which has infinite capacity.

The application of the TDD protocol is used in the network-wide communication protocol [15]. The coherence interval is comprised of four distinct phases, namely uplink training, uplink data transmission, downlink training and downlink data transmission that is displayed in Figure 2. Furthermore, the model is implemented with the underlying assumption that all ARSs efficiently serve users by utilizing the same time-frequency resource concurrently. Depending on the needs of the system, there are many different strategies for selecting the active ARS set.

Then we introduce a new SC model based on the CF model. In this model, instead of multiple ARS being

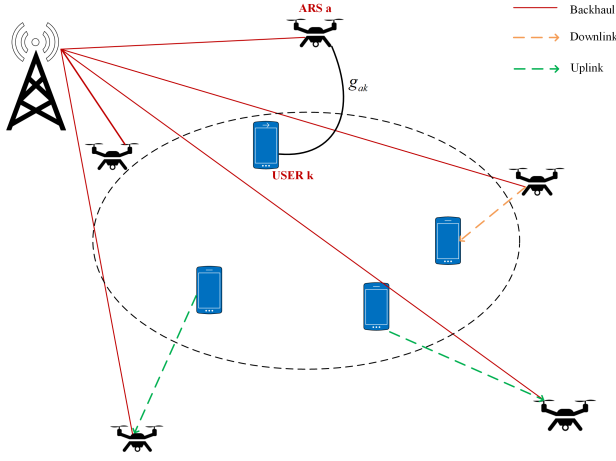


Figure 1. The system model of multi-ARS SC.

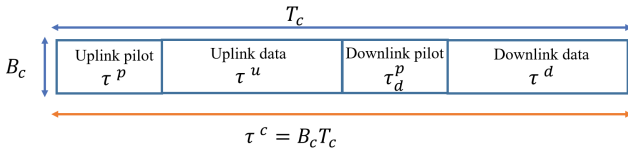


Figure 2. Time-division duplex (TDD) protocol.

activated to serve users, each user selects only one suitable ARS to communicate with at a certain time. Therefore, in contrast to CF Massive MIMO, the channel in SC systems does not harden [16]. That is the reason for the need to have channel estimation in both uplink and downlink, so the coherence interval must include a total of four phases. We denote τ^c to be the coherence interval length in frequency-time samples at which the channel is stable, τ^p is the length of the uplink training phase with $\tau^p \leq \tau^c$. τ^u and τ^d are the uplink and downlink transmission intervals, respectively.

The channel is affected by both small-scale fading and large-scale fading. Large-scale fading in the deployment scenario where ARSs are located at a relatively high altitude is mainly affected by path loss. During each coherence interval, the small-scale fading is assumed to remain static, while changing independently from one coherence interval to the next. On the other hand, the large-scale fading exhibits a much slower rate of change and remains constant for several coherence intervals [17].

In this work, the channel coefficient vector between a th ARS and k th user is illustrated by $\mathbf{g}_{ak} \in \mathbb{C}^{M \times 1}$. Channel coefficient vector is determined as follows [18]

$$\mathbf{g}_{ak} = \sqrt{\beta_{ak}} \mathbf{h}_{ak}, \quad (1)$$

where β_{ak} is the large-scale fading coefficient and $\mathbf{h}_{ak} \in \mathbb{C}^{M \times 1}$ is a small-scale fading vector that is independently and identically distributed (i.i.d.) $\mathcal{CN}(0, \mathbf{I}_M)$ random variable (RV) vectors.

The value of β_{ak} is determined by the path loss between the ARSs and the intended users. Large-scale fading coefficient β_{ak} is written as [18]

$$\beta_{ak} = 10^{-\frac{\text{PL}_{ak}}{10}}, \quad (2)$$

where PL_{ak} denotes the path loss in decibels. In this paper, we consider PL_{ak} in the urban micro (UMi) scenario, which is provided based on the 3GPP standard support for aerial vehicle at [14, Table B-2]

$$\text{PL}_{ak} = \begin{cases} \text{PL}_{\text{LoS}} = \max \{ \text{PL}', 30.9 + (22.25 - 0.5 \log_{10}(h_{\text{ARS}})) \log_{10}(d_{3D}) + 20 \log_{10}(f_c) \} \\ \text{PL}_{\text{NLoS}} = \max \{ \text{PL}_{\text{LoS}}, 32.4 + (43.2 - 7.6 \log_{10}(h_{\text{ARS}})) \log_{10}(d_{3D}) + 20 \log_{10}(f_c) \}, \end{cases} \quad (3)$$

where PL' , PL_{LoS} , and PL_{NLoS} indicate respectively the free space path loss, LoS/NLoS path loss of ARSs in the UMi situation. f_c is the carrier frequency and the height of ARS is h_{ARS} with $22.5\text{m} \leq h_{\text{ARS}} \leq 300\text{m}$. d_{3D} is the three-dimensional distance between the ARS and users.

In comparison with the ground-based CF model, the communication channel between ARSs and users in the ARSs-based system is generally better. The reason is that LoS is consistently present in communication, and shadow fading also can be disregarded in this scenario. Additionally, unlike the ground-based CF models, the ARSs-based model can be deployed flexibly and easily, which makes our model suitable for several specific communication scenarios such as search and rescue, smart cities, disaster recovery, etc.

Compared with the Multi-ARS CF model, the Multi-ARS SC model is more energy-saving and has a lower backhaul overload probability. Moreover, the ARS selection algorithms, power optimization algorithms, and signal processing in the Multi-ARS SC model is much simpler.

3 ARS SELECTION AND UPLINK DATA TRANSMISSION

3.1 ARS Selection

In the SC systems, each user is served exclusively by a single ARS at a certain time. The criterion for the selection is that ARSs select the user with the highest average received useful signal power, the k th user is only linked to the ARS with the largest large-scale fading coefficients. That is completely reasonable in the context that the channel under consideration is mainly affected by β_{ak} in terms of expectation. Therefore, the channel with the largest β_{ak} coefficient have the best status for efficient communication.

The decisions of the uplink handshake are carried out at each individual ARSs without the need to transmit uplink CSI to the CPU. After the uplink training phase, the ARSs obtained CSI from all users. At each ARSs, all users are sorted in descending order of β_{ak} . The user with the highest β_{ak} is selected to be paired with the ARS. Selected user broadcasts its state information to all of ARSs to announce that it have been selected and the next ARSs need to remove it from the available list. This process is sequentially carried out at all ARSs in the system. We denote k_a is the user chosen by ARS a th

$$k_a \triangleq \max_{k \in \{\text{available users}\}} \beta_{ak}. \quad (4)$$

Thus, to select effectively according to the above plan, the ARS must estimate the channel accurately. The ARS-user pairing process is demonstrated by the algorithm as follows

Algorithm 1 ARS selection

- 1: **Initialization:** Set the selection order of ARSs, $a = 1$.
 - 2: **Find optimal user:** a th ARS finds appropriate user from users set according to β_{ak} .
 - Sort users in descending order of β_{ak} : $\{\beta_{a1}, \beta_{a2}, \dots, \beta_{aK}\} \rightarrow \{\hat{\beta}_{a1}, \hat{\beta}_{a2}, \dots, \hat{\beta}_{aK}\}$ where $\hat{\beta}_{a1} \geq \dots \geq \hat{\beta}_{aK}$
 - Choose a user whose Large scale fading coefficient is determined as: $\max \{\hat{\beta}_{a1}, \hat{\beta}_{a2}, \dots, \hat{\beta}_{aK}\} = \hat{\beta}_{a1}$
 - 3: **Update:** Increase the value of $a \leftarrow a + 1$. If $a \leq A$, return to Step 2. Otherwise, end the algorithm and return the results.
-

The ARS selection algorithm described above is quite simple and achieves local optimality at each ARSs. Successfully addressing the ARS selection problem makes the model simpler in signal processing and power optimization. The algorithm aims to design a flexible SC model that performs well in various scenarios and can be deployed quickly. However, the global optimal has not been well addressed because the result is heavily depended on the order in which ARSs select users.

3.2 Uplink Data Transmission

In the uplink, ARSs initially estimate the channels by utilizing pilots transmitted from users. We use MMSE technique [19] to detect pilot signals during the uplink training phase. In this phase, all users simultaneously send their pilots to ARSs and then ARSs utilize the received pilot data to estimate the channel coefficients. The so-obtained channel estimates are used to detect the desired signals. The pilot sequence from k th user is denoted by $\phi_k \in \mathbb{C}^{\tau^p \times 1}$, assuming $\|\phi_k\|^2 = 1 \forall k$.

The AP that paired with the k th user is symbolized as a_k . The channel coefficients obtained after MMSE estimation can be expressed as follows

$$\hat{\mathbf{g}}_{a_k k} = \mathbf{g}_{a_k k} - \boldsymbol{\varepsilon}_{a_k k}, \quad (5)$$

where $\boldsymbol{\varepsilon}_{a_k k}$ denotes the channel estimation error vector. Due to the properties of MMSE estimation, $\boldsymbol{\varepsilon}_{a_k k}$ is independent of the estimated channel coefficients $\hat{\mathbf{g}}_{a_k k}$. Besides, each element of the estimated channel vector $\hat{\mathbf{g}}_{a_k k}$ is $\mathcal{CN}(0, \omega_{a_k k})$ and each element of $\boldsymbol{\varepsilon}_{a_k k}$ is $\mathcal{CN}(0, \beta_{a_k k} - \omega_{a_k k})$ where

$$\omega_{a_k k} \triangleq \frac{\tau^p \rho^p \beta_{a_k k}^2}{\tau^p \rho^p \sum_{k'=1}^K \beta_{a_k k'} \|\phi_k^H \phi_{k'}\|^2 + 1}. \quad (6)$$

Let ρ^u be the normalized uplink SNR and η_k^u be the power control coefficient at the k th user with $0 \leq \eta_k^u \leq 1$. $\sqrt{\eta_k^u} q_k$, where $\mathbb{E}\{|q_k|^2\} = 1$, is the symbol

of k th user. The expression for the signal acquired at the a_k th ARS can be formulated as

$$\begin{aligned} \mathbf{y}_{a_k}^u &= \sqrt{\rho^u} \sum_{k'=1}^K \mathbf{g}_{a_k k'} \sqrt{\eta_{k'}^u} q_{k'} + \mathbf{w}_{a_k}^u \\ &= \sqrt{\rho^u} \hat{\mathbf{g}}_{a_k k} \sqrt{\eta_k^u} q_k + \sqrt{\rho^u} \boldsymbol{\varepsilon}_{a_k k} \sqrt{\eta_k^u} q_k \\ &\quad + \sqrt{\rho^u} \sum_{k' \neq k}^K \mathbf{g}_{a_k k'} \sqrt{\eta_{k'}^u} q_{k'} + \mathbf{w}_{a_k}^u, \end{aligned} \quad (7)$$

where $\mathbf{w}_{a_k}^u$ is additive Gauss noise. The first term of equation (7) is the desired signal while the second and the third terms are the error in channel estimation, and the interference by other users, respectively. The uncorrelated effective noise can be considered as the last three terms of equation (7) in order to determine the achievable uplink rate for the k th user.

Analyzed $\mathbf{y}_{a_k}^u$ into four components as follows

$$\mathbf{y}_{a_k}^u = D_{a_k} q_k + C_{a_k} q_k + \sum_{k' \neq k}^K I_{kk'} q_{k'} + \mathbf{w}_{a_k}^u \quad (8)$$

where

$$\begin{aligned} D_{a_k} &= \sqrt{\rho^u} \hat{\mathbf{g}}_{a_k k} \sqrt{\eta_k^u} \\ C_{a_k} &= \sqrt{\rho^u} \boldsymbol{\varepsilon}_{a_k k} \sqrt{\eta_k^u} \\ I_{kk'} &= \sqrt{\rho^u} \mathbf{g}_{a_k k'} \sqrt{\eta_{k'}^u} \end{aligned}$$

Therefore, the uplink rate can be calculated at GBS as follows

$$R_k^u = \log_2 \left(1 + \frac{\|D_{a_k}\|^2}{\mathbb{E}\{\|C_{a_k}\|^2\} + \sum_{k' \neq k}^K \mathbb{E}\{\|I_{kk'}\|^2\} + 1} \right) \quad (9)$$

The GBS in the proposed system performs several tasks such as signals receiving and demodulating, resource coordinating, implementing optimization algorithms, etc. As a result, we derive the closed-form equation to calculate the achievable uplink rate as equation (10)

Although the channel is not harden, $\left| [\hat{\mathbf{g}}_{a_k k}]_m \right|^2$ is exponentially distributed with mean $\omega_{a_k k}$ therefore the uplink rate can be expressed in closed form in terms of the exponential integral function $\text{Ei}(\cdot)$ as

$$R_k^u = -(\log_2 e) e^{\frac{1}{\bar{\omega}_{a_k k}}} \text{Ei} \left(-\frac{1}{\bar{\omega}_{a_k k}} \right), \quad (11)$$

where

$$\bar{\omega}_{a_k k} \triangleq \frac{M \rho^u \eta_k^u \omega_{a_k k}}{M \rho^u \eta_k^u (\beta_{a_k k} - \omega_{a_k k}) + M \rho^u \sum_{k' \neq k}^K \eta_{k'}^u \beta_{a_k k'} + 1}. \quad (12)$$

$$R_k^u = \mathbb{E} \left\{ \log_2 \left(1 + \frac{\rho^u \eta_k^u \sum_{m=1}^M [\hat{\delta}_{a_k k}^*]_m [\hat{\delta}_{a_k k}]_m}{M \rho^u \eta_k^u (\beta_{a_k k} - \omega_{a_k k}) + M \rho^u \sum_{k' \neq k}^K \eta_{k'}^u \beta_{a_k k'} + 1} \right) \right\}. \quad (10)$$

Ei(.) is defined at [20, Equation (8.211.1)] as

$$\text{Ei}(x) = - \int_{-x}^{\infty} \frac{e^{-t}}{t} dt = \int_{\infty}^{-x} \frac{e^{-t}}{t} dt = \text{li}(e^x) \quad \text{with } x < 0. \quad (13)$$

4 UPLINK POWER OPTIMIZATION

Transmitting data at the same power at all users is a limited solution that causes many negative impacts on the performance of the system. One of the impacts that we are most concerned is the energy issue of users, especially in the context of users being compact, economical and highly portable mobile devices. Furthermore, uniform transmit power results in high user interference levels. Therefore, we propose the uplink power control algorithm to solve above problems, max-min power control which can be formulated as follows

$$\begin{aligned} & \max_{\{\eta_k^u\}} \min_{k=1, \dots, K} R_k^u \\ & \theta \leq \eta_k \leq 1, \quad \forall k = 1, \dots, K. \end{aligned} \quad (14)$$

Because the value of R_k^u is a monotonically increasing function of $\bar{\omega}_{a_k k}$. Therefore, (14) is equivalent to

$$(\text{P1}) : \max_{\{\eta_k^u\}} \min_{k=1, \dots, K} \bar{\omega}_{a_k k} \quad (15a)$$

$$\theta \leq \eta_k \leq 1, \quad \forall k = 1, \dots, K, \quad (15b)$$

(P1) problem is the maximum problem of $\min_{k=1, \dots, K} \bar{\omega}_{a_k k}$ with respect to the η_k^u variable. To solve the (P1) optimization problem, the objective function and constraints must be linear or quasi-linear. It can be seen that (15b) is a linear function while the objective function in (15a) is not guaranteed to be linear. We transform (15a) equation by using the slack variable t , where t is upper bound of $\min_{k=1, \dots, K} \bar{\omega}_{a_k k}$ [21, Chapter 5, 6]. Therefore, the (P1) problem has an additional constraint as $t \leq \bar{\omega}_{a_k k}$.

Thus, (P1) is rewritten as follows

$$(\text{P2}) : \max_t \quad (16a)$$

$$\{\eta_k^u\}^t \quad (16b)$$

$$t \leq \bar{\omega}_{a_k k}, k = 1, \dots, K \quad (16b)$$

$$0 \leq \eta_k^u \leq 1, k = 1, \dots, K. \quad (16c)$$

The (P2) problem is a quasi-linear program and can be effectively addressed by using a Bisection method [21, p.116].

Algorithm 2 Bisection Algorithm for Solving Quasi-linear Problem

- 1: **Initialization:** Select the initial values of t_{min} and t_{max} , where t_{min} and t_{max} determine a range of relevant values of the objective function in (P2). Define a tolerance value $\epsilon > 0$
- 2: **Solve the feasibility problem** Set $t \leftarrow \frac{t_{min} + t_{max}}{2}$.
 - Solve the feasibility of quasi-linear problem in (P2).
- 3: **Update :** If the problem in (P2) is feasible: set $t_{max} \leftarrow t$, **else:** set $t_{min} \leftarrow t$. **end**
- 4: **Check:** If $t_{max} - t_{min} \leq \epsilon$: Stop and return $\tilde{t} \leftarrow \frac{t_{min} + t_{max}}{2}$. **Else:** return to step 2

The Bisection algorithm divides the interval into two equal parts, gradually reducing the distance between the endpoints to find the optimal point. The Bisection algorithm is a reliable technique for simple functions, providing an approximate solution. The precision depends on the tolerance value, with a smaller tolerance resulting in a closer approximation. However, the consequence is increasing the number of iterations making the system more complex and expand the optimization process.

5 NUMERICAL RESULTS AND DISCUSSIONS

We evaluate the performance of the uplink SC multi-ARS system by comparing the performance of the system with and without power optimization under the impact of varying the relevant parameters such as the total number of ARSs (A), the total number of users (K), the number of antennas at each ARS (M) and uplink pilot length (τ^p). All users and ARSs are randomly and consistently distributed within the same-sized square $S \times S \text{ km}^2$.

5.1 Parameters and Setup

The parameters shown in Table II are utilized in all of the experiments. ARSs are randomly distributed according to a Continuous Uniform Distribution in a 3D space within a $1 \times 1 \text{ km}^2$ area, and the heights range is $22.5m \leq h_{ARS} \leq 300m$. The distance has been clearly expressed and calculated in the Path Loss equation of the channel model (LoS-NLoS). ARS selection strategy based on large-scale fading coefficients is used in this mode. For the case without power control: all users communicate at full power, i.e., $\eta_k^u = 1, k = 1, \dots, K$, while for the case with power control, each user flexibly controls the transmit power based on the power control coefficient. Coefficients are found according to the algorithm presented previously in Section 4. In our

Table II
PARAMETERS OF THE SYSTEM USED FOR SIMULATION

Parameter	Value
Carrier frequency	1.9 GHz
Bandwidth (B)	20MHz
Coherence bandwidth (B_c)	200 KHz
Coherence time (T_c)	1 ms
The noise figure (NF)	9 dB
ARS height	$22.5m \leq h_{ARS} \leq 300m$
ρ^P, ρ^u	100, 100 mW
Coherence interval τ^c	200 samples
Area distribution of ARS and K users (S)	1 km ²

experiments, we have computed the CDF for the uplink throughput of each user. This has been achieved by implementing the specified scenario.

5.2 Results and Discussions

In Figure 3, we illustrates the system performance of the conventional SC model with an AP located on the ground and the SC model with UAVs serving as ARSs. The parameters for both systems are set to be the same: $A = 15, K = 10, L = 1, \tau^P = 10$. The simulation results have clearly demonstrated that the system utilizing UAVs exhibits better performance compared to the conventional SC system. The reason for this improvement is that UAVs flying at higher altitudes provide favorable conditions for better channel transmission, as LoS is consistently present and shadow fading is eliminated.

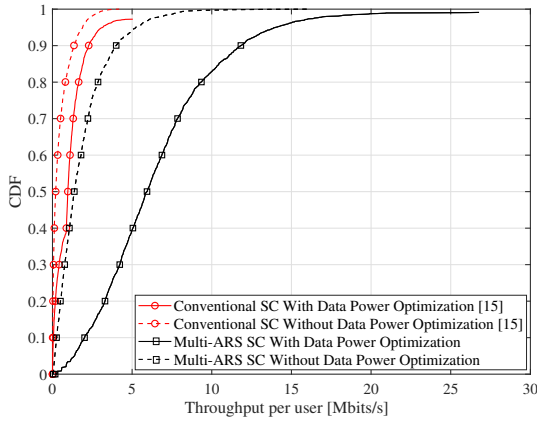


Figure 3. CDFs of the per-user throughput for the cases of conventional SC and Multi-SC SC, $K = 10, A = 15, M = 1$, and $\tau^P = 10$.

In order to highlight more about the impact of the number of users on the performance, we compare the CDF of the per-user uplink throughput with and without uplink data transmission power optimization with parameters $A = 15, M = 1$ and $\tau^P = 10$, and varying $K = 8, 10, 12$ in Figure 4.

It is clear to see that the system with power optimization provides superior performance compared to the system without optimization. Specifically, when $K = 8$, the 90%-likely throughput per user with power optimization is approximately 3.6 Mbits/s. Meanwhile, without for power optimization is 9 times lower at only about 0.4 Mbits/s. The reasonable explanation is that

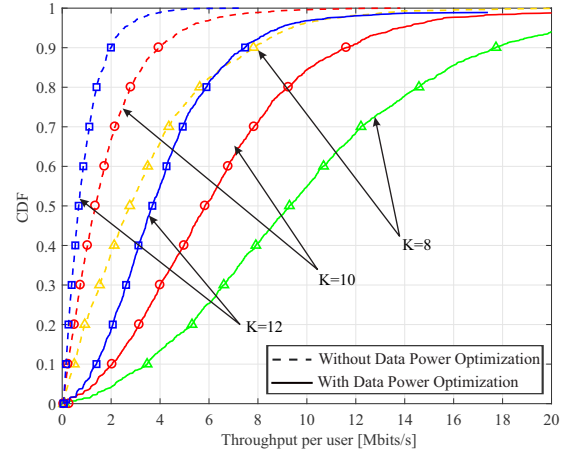


Figure 4. CDFs of the per-user throughput for the cases of uplink data transmission power optimization and without power optimization, $K = 8, 10, 12, A = 15, M = 1$, and $\tau^P = 10$.

in the models without uplink power control have large interference levels at the receiver. Moreover, we also see in Figure 4 that system quality decreases as the number of users increases. The reason is that system performance is evaluated based on per-user throughput instead of total throughput. The smaller the number of users compared to the number of ARS, the greater the possibility of users having a good communication channel. Because there will be additional backup paths for bad channel conditions.

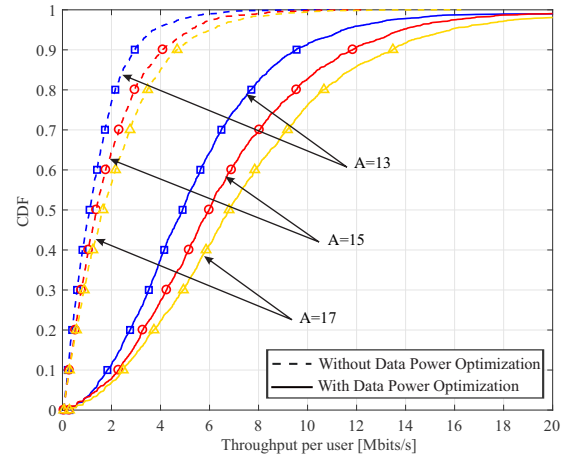


Figure 5. CDFs of the per-user throughput for the cases of uplink data transmission power optimization and without power optimization, $A = 13, 15, 17, K = 10, M = 1$, and $\tau^P = 10$.

Similar conclusions are also demonstrated in Figure 5 with the changed number of ARSs. As A increases, the redundancy in channel selection becomes higher. Therefore, the increasing probability of choosing a good channel increases the overall performance.

In Figure 6, the variation in performances of the systems with the changed number of antennas per ARS M is illustrated. When the number of antennas per ARS increases, the enhancement of diversity gain leads to an improvement in throughput. The larger the number of antennas at each ARS, the more significant

the improvement is made. Specifically, as we can see in Figure 6, the improvement in system performance becomes very obvious with $M = 3$.

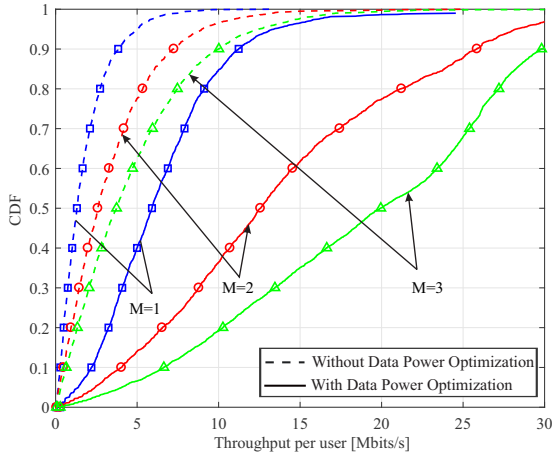


Figure 6. CDFs of the per-user throughput for the cases of uplink data transmission power optimization and without power optimization, $M = 1, 2, 3$, $A = 15$, $K = 10$, and $\tau^p = 10$.

Finally, we demonstrate the impact of pilot length τ^p in Figure 7. Within a certain limit, increasing pilot length helps improve per-user throughput because the channel coefficient is estimated more accurately. As τ^p increases, the number of orthogonal pilots in the pilot set allocated to users increases. The result is that pilot contamination is eliminated, leading to enhancement in the quality of channel estimation and a reduction in coherent interference simultaneously. This improvement is shown to be the largest when raising $\tau^p = 5$ to $\tau^p = 10$. However, when τ^p increases further, the improvement only marginally enhances. For example, $\tau^p = 20$ and $\tau^p = 25$ show quite similar performance. The reason is that when the pilot interval is excessively long, it consequently shortens the uplink data interval, leading to a reduction in data throughput.

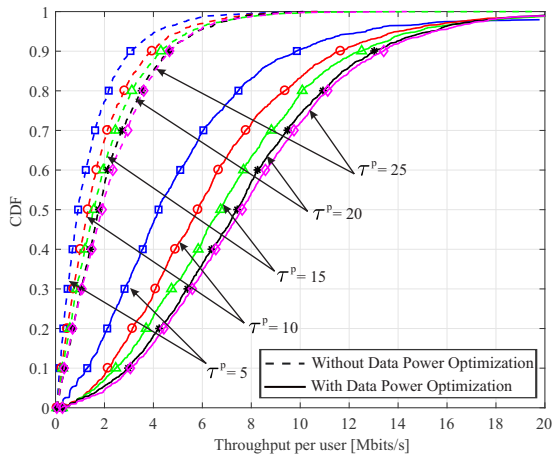


Figure 7. CDFs of the per-user throughput for the cases of uplink data transmission power optimization and without power optimization, $\tau^p = 5, 10, 15, 20, 25$, $A = 15$, $K = 10$, and $M = 1$.

6 CONCLUSION

In this paper, we introduced the Multi-ARS SC model with ARSs and users located randomly in a specific area. The proposed model achieves better performance than conventional ground-based SC systems. Moreover, the power optimization algorithm has also been applied in our model to enhance total system performance. The performance evaluation of the suggested system was conducted in multiple scenarios with different numbers of ARS, numbers of antennas at each ARS, numbers of served users and length of pilot intervals. The results show that the power optimization algorithm gives superior performance. The pairing of the ARS and user in the uplink is performed at the ARS based on the principle of the highest large-scale fading coefficient. The proposed ARS selection Algorithm is simple and achieves local optimality. However, the global optimal has not been well addressed. Therefore, several more optimal selection algorithms will be investigated in the future works.

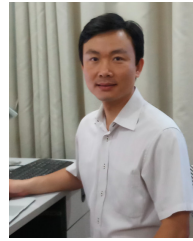
ACKNOWLEDGMENT

This research is funded by Vietnam National Foundation for Science and Technology Development (NAFOSTED) under grant number 102.02-2021.56.

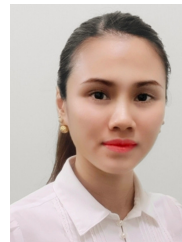
REFERENCES

- [1] D. Pliatsios, S. K. Goudos, T. Lagkas, V. Argyriou, A.-A. A. Boulgeorgos, and P. Sarigiannidis, "Drone-based station for next-generation internet-of-things: A comparison of swarm intelligence approaches," *IEEE Open Journal of Antennas and Propagation*, vol. 3, pp. 32–47, 2021.
- [2] M. H. Alsharif and R. Nordin, "Evolution towards fifth generation (5G) wireless networks: Current trends and challenges in the deployment of millimetre wave, massive MIMO, and small cells," *Telecommunication Systems*, vol. 64, pp. 617–637, 2017.
- [3] A. Abrol and R. K. Jha, "Power optimization in 5G networks: A step towards green communication," *IEEE Access*, vol. 4, pp. 1355–1374, 2016.
- [4] Y. Pak, K. Min, and S. Choi, "Performance evaluation of various small-cell deployment scenarios in small-cell networks," in *Proceedings of the 18th IEEE International Symposium on Consumer Electronics (ISCE 2014)*. IEEE, 2014, pp. 1–2.
- [5] J. Chen, X. Ge, and Q. Ni, "Coverage and handoff analysis of 5G fractal small cell networks," *IEEE Transactions on Wireless Communications*, vol. 18, no. 2, pp. 1263–1276, 2019.
- [6] J. Tanveer, A. Haider, R. Ali, and A. Kim, "An overview of reinforcement learning algorithms for handover management in 5G ultra-dense small cell networks," *Applied Sciences*, vol. 12, no. 1, p. 426, 2022.
- [7] D. C. Nguyen, M. Ding, P. N. Pathirana, A. Seneviratne, J. Li, D. Niyato, O. Dobre, and H. V. Poor, "6G Internet of Things: A comprehensive survey," *IEEE Internet of Things Journal*, vol. 9, no. 1, pp. 359–383, Aug. 2022.
- [8] B. Alzahrani, O. S. Oubbati, A. Barnawi, M. Atiquzzaman, and D. Alghazzawi, "UAV assistance paradigm: State-of-the-art in applications and challenges," *Journal of Network and Computer Applications*, vol. 166, p. 102706, 2020.

- [9] X. Li, Q. Wang, Y. Liu, T. A. Tsiftsis, Z. Ding, and A. Nalathan, "UAV-aided multi-way NOMA networks with residual hardware impairments," *IEEE Wireless Communications Letters*, vol. 9, no. 9, pp. 1538–1542, 2020.
- [10] B. Li, S. Zhao, R. Miao, and R. Zhang, "A survey on unmanned aerial vehicle relaying networks," *IET Communications*, vol. 15, no. 10, pp. 1262–1272, 2021.
- [11] K. Messaoudi, O. S. Oubbati, A. Rachedi, A. Lakas, T. Bendouma, and N. Chaib, "A survey of UAV-based data collection: Challenges, solutions and future perspectives," *Journal of Network and Computer Applications*, p. 103670, 2023.
- [12] M. A. Ouamri, D. Singh, M. A. Muthanna, A. Bounceur, and X. Li, "Performance analysis of UAV multiple antenna-assisted small cell network with clustered users," *Wireless Networks*, vol. 29, no. 4, pp. 1859–1872, 2023.
- [13] B. A. Duc, T. M. Hoang, N. T. Phuong, X. N. Tran, and P. T. Hiep, "Optimizing power for data transmissions in uplink cell-free multi-ABSs communication systems," in *Proceedings of the 2022 International Conference on Advanced Technologies for Communications (ATC)*. IEEE, Nov. 2022, pp. 23–28.
- [14] 3GPP, "Technical specification group radio access network; study on enhanced LTE support for aerial vehicles," *TR 36.777*, Dec 2017.
- [15] H. Q. Ngo, A. Ashikhmin, H. Yang, E. G. Larsson, and T. L. Marzetta, "Cell-free massive MIMO versus small cells," *IEEE Transactions on Wireless Communications*, vol. 16, no. 3, pp. 1834–1850, 2017.
- [16] T. L. Marzetta and H. Yang, *Fundamentals of massive MIMO*. Cambridge University Press, 2016.
- [17] A. Ashikhmin, T. L. Marzetta, and L. Li, "Interference reduction in multi-cell massive MIMO systems I: Large-scale fading precoding and decoding," *ArXiv*, vol. abs/1411.4182, 2014.
- [18] S. Buzzi and C. D'Andrea, "Cell-Free Massive MIMO: User-Centric Approach," *IEEE Wireless Communications Letters*, vol. 6, no. 6, pp. 706–709, Aug. 2017.
- [19] M. K. Steven, "Fundamentals of statistical signal processing," *PTR Prentice-Hall, Englewood Cliffs, NJ*, vol. 10, no. 151045, p. 148, 1993.
- [20] I. S. Gradshteyn and I. M. Ryzhik, *Table of integrals, series, and products*. Academic press, 2014.
- [21] E. K. Chong, W.-S. Lu, and S. H. Zak, *An introduction to optimization*. John Wiley & Sons, 2023.



Pham Thanh Hiep received a B.E. degree in Communications Engineering from National Defence Academy, Japan, in 2005; received the M.E. and Ph.D. degrees in Physics, Electrical, and Computer Engineering from Yokohama National University, Japan, in 2009 and 2012, respectively. He was working as an associate researcher at Yokohama National University, Yokohama, Japan from 2012 to 2015. Now, he is a lecturer at Le Quy Don Technical University, Ha Noi, Viet Nam. Prof. Hiep was a recipient of the best paper from The 25th National Conference on Electronics, Communications and Information Technology, and a co-recipient of the student best paper from The 2022 International Conference on Advanced Technologies for Communications. His research interests lie in the area of wireless communication technologies and signal processing. His research interests lie in the area of wireless communication and signal processing technologies.



Nguyen Thu Phuong received the B.S, M.S and PhD degrees from Le Quy Don Technical University, Vietnam in 2008, 2012 and 2016, respectively. She is now a lecturer at Faculty of Radio-Electronics Engineering, and a significant member of the Advanced Wireless Communication Group, Le Quy Don Technical University, Hanoi, Vietnam. Her research interests are in the area of emerging technologies for future wireless communications: Energy harvesting, Non-orthogonal multiple access (NOMA), space-time processing, space-time coding, spatial modulation and index modulation, and massive MIMO systems.



Be Thi Bich Hoai was born in April 12, 1998. She received the B.S degree from Le Quy Don Technical University in 2021. She currently is a M.S student at Le Quy Don Technical University, Hanoi, Vietnam. Her research interests are in the area of MIMO systems, spatial modulation, Small-Cell and Cell-Free models.



Bui Anh Duc was born in August 22, 1989. He received a B.S. degree in Communication Command at Telecommunications University, Ministry of Defense, Vietnam, in 2011, and an MS degree from Le Quy Don Technical University, Vietnam in 2017. He is currently pursuing a Ph.D degree at Le Quy Don Technical University, Hanoi, Vietnam. His research interests include unmanned aerial vehicle communications, MIMO and Cell Free Massive MIMO systems, and signal processing for wireless cooperative communications. He was a recipient of the IEEE ATC2022 Best Paper Award.

ing for wireless cooperative communications. He was a recipient of the IEEE ATC2022 Best Paper Award.